

## BOUNDARY PROBLEMS IN DD SIMULATIONS

B. DEVINCRE<sup>1</sup>, A. ROOS<sup>2</sup> AND S. GROH<sup>1</sup>

<sup>1</sup>*LEM, CNRS-ONERA, 29 av. de la division Leclerc, 92322 Chatillon Cedex, France*

<sup>2</sup>*DMSE/LCME, ONERA, 29 av. de la division Leclerc, 92322 Chatillon Cedex, France*

**Abstract.** Over the years, different approaches have been developed to calculate the state of mechanical equilibrium in a dislocated finite body. The purpose of this paper is to show the common aspects among the approaches used with Dislocation Dynamics simulations, as well as their distinctive features. Given the uniqueness of the solution, an attempt is made to explicitly illustrate how it is translated within the different existing frameworks. Two approaches are distinguished according to whether the stress singularity along the dislocations lines is homogenized or not. It is shown that the solution to be preferred depends on the problems at hand.

### 1. Introduction

Over the years, different methods have been developed to calculate the state of mechanical equilibrium in a dislocated finite body. Recently, such studies were found to be useful for the development of exact 3D simulations of dislocation dynamics (DD). In this paper, a critical review of the existing numerical solutions is carried out. Such solutions are based on the *superposition method* [1, 2, 3, 4] and the *Discrete-Continuous Model* (DCM) [5, 6]. Although the underlying physical problem is the same, and therefore also its mechanical solution, these methods follow different strategies. As a consequence, it is not always clear how and where exactly they differ or are similar. Our purpose is here to establish their common features and their differences in a concise manner, as well as to determine their preferential domain of application. By lack of space, the case of simulations making use of periodic boundary conditions, as well as the recent phase-field approaches used to model dislocation dynamics, are not considered.

Throughout this study, use is made of normal type ( $a$ ) to denote scalar quantities and of bold characters ( $\mathbf{a}$ ) for vectors. Second order tensors are underlined ( $\underline{a}$ ), and fourth order tensors are doubly underlined  $\underline{\underline{a}}$ .

## 2. Statement of the problem

### 2.1. DISLOCATIONS IN A CONTINUUM MEDIUM

Following the seminal work of Mura [7], dislocations can be regarded as line defects causing eigenstresses in an elastic medium. For each dislocation, a volume  $C$  is defined, which surrounds the line and its slip trace (see figure 1). Within this volume (of penny shape with constant thickness  $h$  in the direction  $\mathbf{n}$ , normal to the dislocation slip plane) an eigenstrain field,  $\underline{\varepsilon}^p$ , exists that leaves into the medium a plastic deformation in the form of a displacement shift (or shear). The direction and the magnitude of this plastic shear are characterized by the Burgers vector,  $\mathbf{b}$ . Outside  $C$  and at the boundary  $\partial C$ , the eigenstrain  $\underline{\varepsilon}^p$  is by definition equal to zero. When a small volume element  $v$  included in  $V$  is sheared by several dislocation segments  $i$ , the associated eigenstrain is denoted by  $\underline{\varepsilon}_v^p = \sum_i \underline{\varepsilon}^{p,i}$ . One must realize that the dislocation core properties are not accounted for in this framework, but this is not a problem in what follows since the dislocation core structure has a weak influence on the boundary value problem.

In a few ideal cases, such as dislocations in an infinite elastic medium and with a Heaviside step function as eigenstrain solution, the mechanical problem of the equilibrium state of a dislocated body can be solved analytically. This development is reported in many textbooks (see for instance [7]) and is, therefore, not be reproduced here. One must only keep in mind that the solutions for  $\underline{\sigma}^\infty$  and  $\underline{\varepsilon}^\infty$  are relatively simple and are commonly used to predict the elastic properties of dislocations [8].

### 2.2. MECHANICAL EQUILIBRIUM IN A FINITE BODY

Van der Giessen and Needleman [1] were the first to emphasize the importance of the boundary value problem in mesoscopic simulations of plastic deformation. Indeed, DD codes, in their standard formulation, use for reason of simplicity and code efficiency analytical forms justified only in an isotropic infinite body. When a finite body is concerned, or when there are internal interfaces, this simple solution is *a priori* no longer valid and the true boundary value problem (BVP) has to be solved.

Consider, as in figure 1, a computational volume  $V$ , which may contain elastic inclusions of volume  $V^*$  and dislocations (line segments  $i$ ) in a matrix phase  $V^M = V - V^*$ . The elastic properties of the matrix are governed by the fourth-order tensor  $\underline{\underline{L}}^M$ , while the elastic modulus tensor of the inclusion

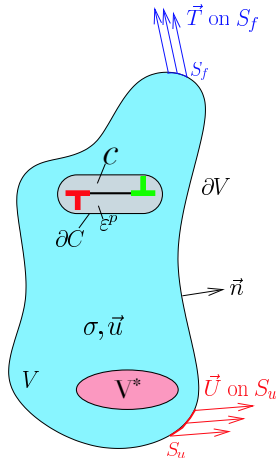


Figure 1. Statement of the mechanical problem. A description of all quantities can be found in the text. In mechanical equilibrium all fields must satisfy equation (1).

is denoted  $\underline{\underline{L}}^*$ . Tractions  $\mathbf{T}$  can be prescribed at the boundary  $S_f$ , and displacements  $\mathbf{U}$  at the boundary  $S_u$ . The latter may also include a plastic displacement  $\mathbf{u}^p$  induced by dislocations that moved out of the volume  $V$  in an earlier deformation stage. The outward normal to the surface is denoted by  $\mathbf{n}$ .

In the absence of overall body forces, the equilibrium state of the total volume is described by the stress field  $\sigma$  and the total strain field  $\underline{\varepsilon}$  that must satisfy:

$$\left\{ \begin{array}{lcl} \nabla \cdot \underline{\sigma} & = & \mathbf{0} \\ \underline{\sigma} \cdot \mathbf{n} & = & \mathbf{T} \text{ at } S_f \\ \mathbf{u} & = & \mathbf{U} \text{ at } S_u \\ \nabla \mathbf{u} & = & \underline{\varepsilon} \\ \underline{\sigma} & = & \underline{\underline{L}}^M : (\underline{\varepsilon} - \underline{\varepsilon}^p) \text{ in } V^M \\ \underline{\sigma} & = & \underline{\underline{L}}^* : \underline{\varepsilon} \text{ in } V^* \end{array} \right. \quad (1)$$

### 3. Solution strategies for DD simulations

Depending upon the precision required and on the nature of the problem to be solved, different numerical methods are available for computing field that satisfy equations (1). Two approaches are particularly well adapted to DD simulations and have been the object of several applications. Both of them make use of a coupling with a Finite Element (FE) code, but the resolution of the algebraic equations involved is not attached to any particular method.

For instance, Boundary Elements, Finite Volume or Element Free Galerkin methods could be a good alternative to the classical FE approach.

### 3.1. THE DISCRETE-CONTINUOUS MODEL

The Discrete-Continuous Model (DCM) was the first solution effectively used in conjunction with 3D simulations of dislocation dynamics [5, 6]. In this method, a FE code computes directly the displacement field satisfying equations (1), making use of the plastic strain,  $\underline{\varepsilon}^p$ , yielded by the DD simulation. Thus the DD code serves as a substitute for the constitutive form used in standard FE frameworks. The most difficult part of the coupling consists in setting conditions that leave the possibility for the FE mesh to capture the complexity of the elastic fields involved during plastic deformation. Two important steps of the computational method must be distinguished: a homogenization procedure for the calculation of  $\underline{\varepsilon}^p$  and an interpolation procedure for the calculation of  $\underline{\sigma}$ .

The homogenization procedure is certainly the most critical part of the method, and a publication has been dedicated to it[9]. In consistency with the framework recalled in § 2.1, the plastic shear associated with the motion of dislocations is extended over a slab of thickness  $h$ . This is formally equivalent to replacing one dislocation by a continuum distribution of parallel infinitesimal dislocations, or to distributing the eigenstrains  $\underline{\varepsilon}^{p,i}$  of each dislocation  $i$  over a large slab, rather than on an infinitely thin plate. Within the slab of typical thickness  $h = 3 v_G^{1/3}$  ( $v_G$  is the elementary volume associated to the Gauss points in the FE mesh), the Burgers vector can be split linearly or with the help of a shape function that helps localizing the dislocation slip plane in the FE mesh. In what follows, only the linear solution will be considered for the sake of simplicity, although a polynomial solution is preferred in the practice.

When a dislocation segment  $i$  belonging to the slip system of normal  $\mathbf{n}$  and Burgers vector  $\mathbf{b}^i$  moves, it generates increments of resolved plastic shear. These increments,  $\Delta\gamma_{n,e}^i$ , are homogenized within the elementary volumes  $v_{G,e}$  of the Gauss points  $e$  according to:

$$\Delta\gamma_{n,e}^i = \frac{(b^i/h)v_{int,e}^i}{v_{G,e}} \quad (2)$$

where  $v_{int,e}^i$  is the volume of intersection between the sheared slab of segment  $i$  and a volume  $v_{G,e}$ . Notice that  $C^i$  and  $v_{int,e}^i$  are related by:

$$C^i = \sum_e v_{int,e}^i \quad (3)$$

Then, the plastic strain increment at each Gauss point of the FE mesh is the sum of the contributions of all the segments  $i$  of unit shear direction  $\mathbf{l}^i = \mathbf{b}^i/b^i$  and moving in  $v_{G,e}$ :

$$\Delta\underline{\varepsilon}_{,e}^p = \sum_i \Delta\gamma_{n,e}^i (\mathbf{l}^i \otimes \mathbf{n}^i)^{sym} \quad (4)$$

Finally, to obtain the total plastic strain at step  $k$ , the sum of all increments from step 0 to step  $k$  is needed:

$$\underline{\varepsilon}_{,e}^p = \sum_0^k \Delta\underline{\varepsilon}_{,e}^p \quad (5)$$

Once  $\underline{\varepsilon}^p$  is defined at each Gauss point of the FE mesh, the problem of the equilibrium state (Eq. 1) can be solved in a conventional manner. The only modification made with respect to an ordinary FE explicit scheme is that the increments of total deformation  $\Delta\underline{\varepsilon}_{,e}$  need to be computed simultaneously everywhere in the FE mesh. This modification is necessary for the DD simulation.

The second critical procedure of the DCM is the interpolation step. This operation is not specific to the DCM and exists in the other approach discussed below. Nevertheless, this procedure is more critical in the DCM case where the FE mesh is strongly deformed. To compute the Peach-Kohler force on each dislocation, the stresses calculated at the Gauss points,  $\underline{\sigma}_{,e}$ , must be interpolated at reference points along the dislocation line. The quality of this interpolation strongly influences the dynamics of the dislocations. It is directly related to the flexibility offered by the polynomial shape functions associated with the FE mesh. For this reason, mesh elements containing a large number of nodes and Gauss points are required. Typically, the DCM calculations make use of elements consisting of 20 nodes - 27 Gauss points.

### 3.2. THE SUPERPOSITION METHOD

This approach was first used by Van der Giessen and Needleman [1] for 2-D simulations, but is now applied to 3-D simulations [2, 3, 4]. The basic objective of this method is to enable an accurate description of the dislocation-dislocation interactions at short distances, while, at the same time, simplifying as much as possible the computations delivered to the FE code. In rough terms, the idea is to eliminate from the FE mesh the elastic singularity associated to the dislocation fields. This can be done by extracting the singular solutions for dislocations in an infinite body,  $\underline{\sigma}^\infty$  and  $\mathbf{u}^\infty$  (see § 2.1) from the whole mechanical problem.

More precisely, the simulated problem (cf. fig. 1) is decomposed into two sub-problems. The first sub-problem is that of interacting dislocations in a homogeneous, isotropic, infinite solid, the  $(\sim)$  fields, and the second one is the complementary problem of accounting for the initial non-homogeneous body, but without dislocations and with modified boundary conditions, the  $(\wedge)$  fields. The state of the simulated body is then re-written as the superposition of two fields:

$$\begin{aligned}\mathbf{u} &= \widehat{\mathbf{u}} + \widetilde{\mathbf{u}} \\ \underline{\varepsilon} &= \widehat{\underline{\varepsilon}} + \widetilde{\underline{\varepsilon}} \\ \underline{\sigma} &= \widehat{\underline{\sigma}} + \widetilde{\underline{\sigma}}\end{aligned}\tag{6}$$

Note that the fields of the  $(\sim)$  sub-problem may be decomposed again into two contributions:

$$\begin{aligned}\widetilde{\mathbf{u}} &= \mathbf{u}^\infty + \mathbf{u}^b \\ \widetilde{\underline{\varepsilon}} &= \underline{\varepsilon}^\infty + \underline{\varepsilon}^b \\ \widetilde{\underline{\sigma}} &= \underline{\sigma}^\infty\end{aligned}\tag{7}$$

where the additional fields  $\mathbf{u}^b$  and  $\underline{\varepsilon}^b$  exist only at the boundary and account for the body shape transformation. Indeed, each time a dislocation moves out of the finite body, it vanishes at the surface leaving a step of magnitude  $b$ , and the shape of the finite body is changed. Accounting for this dislocation-boundary interaction is one of the most difficult parts of the superposition method. Among possible solutions, the concept of virtual dislocations developed by Weygand *et al.* [10] is extremely useful. To avoid the computation of  $\mathbf{u}^b$  and  $\underline{\varepsilon}^b$ , it is suggested that the outgoing dislocations should never be eliminated, but accumulated outside the simulated body, at virtual coordinates consistent with the dislocation slip planes. The benefit of that procedure is that displacements at the boundary are computed in the same manner as in the volume.

Then, the governing equations for the  $(\sim)$  fields are, by construction, free of boundary conditions and can be summarized as follows:

$$\left\{ \begin{array}{l} \nabla \cdot \widetilde{\underline{\sigma}} = \mathbf{0} \\ \widetilde{\underline{\sigma}} = \underline{\underline{L}} : \widetilde{\underline{\varepsilon}} \\ \widetilde{\underline{\varepsilon}} = \nabla \widetilde{\mathbf{u}} \end{array} \right. \quad \text{in } V = V^M \cup V^* \tag{8}$$

With the help of equations (1), (6) and (8), we can now define the equations governing the sub-problem for the  $(\wedge)$  fields:

i) in  $V$

$$\begin{aligned} \nabla \cdot \underline{\sigma} = \mathbf{0} &\iff \nabla \cdot (\widehat{\underline{\sigma}} + \widetilde{\underline{\sigma}}) = \nabla \cdot \widehat{\underline{\sigma}} + \nabla \cdot \widetilde{\underline{\sigma}} = \nabla \cdot \widehat{\underline{\sigma}} \\ &\Rightarrow \nabla \cdot \widehat{\underline{\sigma}} = \mathbf{0} \end{aligned} \quad (9)$$

and

$$\begin{aligned} \underline{\varepsilon} = \widehat{\underline{\varepsilon}} + \widetilde{\underline{\varepsilon}} = \nabla \mathbf{u} &\iff \underline{\varepsilon} - \widetilde{\underline{\varepsilon}} = \nabla \mathbf{u} - \nabla \widetilde{\mathbf{u}} \\ &\Rightarrow \widehat{\underline{\varepsilon}} = \nabla \widehat{\mathbf{u}} \end{aligned} \quad (10)$$

ii) at the boundary we have on  $S_f$ :

$$\begin{aligned} \underline{\sigma} \cdot \mathbf{n} = \mathbf{T} &\iff \widehat{\underline{\sigma}} \cdot \mathbf{n} = \mathbf{T} - \widetilde{\underline{\sigma}} \cdot \mathbf{n} \\ &\Rightarrow \widehat{\underline{\sigma}} \cdot \mathbf{n} = \mathbf{T} - \widetilde{\mathbf{T}} \end{aligned} \quad (11)$$

and on  $S_u$ :

$$\begin{aligned} \mathbf{u} &= \widehat{\mathbf{u}} + \widetilde{\mathbf{u}} = \mathbf{u}^{app} \\ &\Rightarrow \widehat{\mathbf{u}} = \mathbf{u}^{app} - \widetilde{\mathbf{u}} \end{aligned} \quad (12)$$

iii) finally, keeping in mind that  $\underline{\varepsilon}^p$  is non-zero only inside  $C$  and that the thickness of  $C$  tends to zero when the analytical solutions hold, we have in  $V^M$ :

$$\begin{aligned} \underline{\sigma} = \underline{\underline{L}} : (\underline{\varepsilon} - \underline{\varepsilon}^p) &= \underline{\underline{L}} : (\widehat{\underline{\varepsilon}} + \widetilde{\underline{\varepsilon}} - \underline{\varepsilon}^p) = \underline{\underline{L}} : (\widehat{\underline{\varepsilon}} + \widetilde{\underline{\varepsilon}}) = \underline{\underline{L}} : \widehat{\underline{\varepsilon}} + \widetilde{\underline{\sigma}} \\ &\Rightarrow \widehat{\underline{\sigma}} = \underline{\underline{L}} : \widehat{\underline{\varepsilon}} \end{aligned} \quad (13)$$

and in  $V^*$ :

$$\begin{aligned} \underline{\sigma} = \widehat{\underline{\sigma}} + \widetilde{\underline{\sigma}} &= \underline{\underline{L}}^* : \underline{\varepsilon} = \underline{\underline{L}}^* : (\widehat{\underline{\varepsilon}} + \widetilde{\underline{\varepsilon}}) \\ &\Rightarrow \widehat{\underline{\sigma}} = \underline{\underline{L}}^* : \widehat{\underline{\varepsilon}} + (\underline{\underline{L}}^* - \underline{\underline{L}}) : \widetilde{\underline{\varepsilon}} \end{aligned} \quad (14)$$

In summary, the equilibrium state equations for the ( $\wedge$ ) sub-problem are:

$$\left\{ \begin{array}{lcl} \nabla \cdot \widehat{\underline{\sigma}} &=& \mathbf{0} \\ \widehat{\underline{\sigma}} \cdot \mathbf{n} &=& \mathbf{T}^{app} - \underline{\sigma}^\infty \cdot \mathbf{n} \quad \text{at } S_f \\ \widehat{\mathbf{u}} &=& \mathbf{U}^{app} - \widetilde{\mathbf{u}} \quad \text{at } S_u \\ \nabla \widehat{\mathbf{u}} &=& \widehat{\underline{\varepsilon}} \\ \widehat{\underline{\sigma}} &=& \underline{\underline{L}} : \widehat{\underline{\varepsilon}} \quad \text{in } V^M \\ \widehat{\underline{\sigma}} &=& \underline{\underline{L}}^* : \widehat{\underline{\varepsilon}} + (\underline{\underline{L}}^* - \underline{\underline{L}}) : \widetilde{\underline{\varepsilon}} \quad \text{in } V^* \end{array} \right. \quad (15)$$

By resolving this elastic problem with a FE meshing, and adding the analytical solutions of the ( $\sim$ ) fields problem to that solution, i.e. by adding  $\sigma^\infty$ ,  $\varepsilon^\infty[+\varepsilon^b]$  and  $\mathbf{u}^\infty[+\mathbf{u}^b]$ , one can determine solutions for the total problem as defined in equations (1).

#### 4. Discussion

In this section the strengths and weaknesses of the BVP solutions presented in §3 are compared. The discussion is based on the authors' recent evaluations and validation tests. We tried, as much as possible, to restrict our comments to general features independent of the coding details of the simulations.

In terms of CPU, the comparison of the DCM and the superposition method is usually in favor of the last one. Indeed, as mentioned in §3.1, the DCM requires a more detailed meshing (i.e. more elements with many nodes and Gauss points) and, therefore, larger computations. Also, the superposition method requires only data transfer between the DD and FE codes at the boundary elements of the mesh, whereas, the DCM imposes data transfer everywhere. From a practical viewpoint, the implementation of DD-FE coupling based on the superposition approach is easier to realize, but this last point may depend on the FE code that is used. From a theoretical point of view, the two approaches are perfectly equivalent with one exception; calculations in an elastically anisotropic medium can be realized much more easily using the DCM approach. Indeed, for the superposition solution to be efficient, analytical forms are required for the displacement field of dislocation segments and for anisotropic media a general solution does not exist. In contrast, elastic anisotropy is easily taken into account with the DCM by only changing one input of the DCM calculation: the tensor of elastic moduli of the considered material. As a result, computing times are virtually the same for isotropic and anisotropic simulations.

To obtain the stress at an arbitrary position in the simulated body, FEs are using shape functions which interpolate the stresses calculated at Gauss points. A basic hypothesis of the classical FE method imposes that these shape functions are continuous within the elements. Since the dislocation fields vary as the inverse of the distance to the line, the resulting singularities at the dislocation line cannot be exactly accounted for. For instance, our tests show that quadratic elements (i.e. with a polynomial shape function of order two) become inaccurate at distances from a dislocation line of the order of  $v_G^{1/3}$ . This is why, without correction, the DCM cannot precisely account for dislocation-dislocation contact and short distance interactions. An immediate solution to this problem consists in refining the mesh and, consequently, decreasing the homogenization thickness  $h$  around the dislocation lines. The latter is directly linked to the size of finite element mesh and to  $v_G$ . However, this leads rapidly to useless simulations in term of computation times, especially in 3D. Alternatively, we can use in the DCM analytical forms for segment-segment elastic interactions at short distances (i.e. when two segments are at a distance smaller than  $1.7 v_G^{1/3}$ ).

This additional force contribution to the dislocation dynamics simulation can be regarded as a constitutive rule caring of the lack of accuracy of the FE mesh at short distance.

It is interesting to note that the above problem of the DCM approach turns into an advantage when dislocation segments are close to boundaries. Indeed, in the superposition approach the boundary conditions on  $S_f$  and/or  $S_u$  contain an image contribution proportional to minus  $\sigma^\infty$  and  $\mathbf{u}^\infty$ , respectively. When a dislocation approaches the boundary, these contributions diverge, and in fact become infinite when dislocations touch a Gauss point at the boundary. To precisely account for this surface effect requires an accurate subtraction of the large ( $\sim$ ) and ( $\wedge$ ) fields, hence a remeshing of the boundaries close to the points where segments are emerging [11]. Without such a procedure, important errors arise on the amplitude of the image force (the nodes at the surface elements cannot accommodate the important elastic displacement imposed by the emerging dislocations). To the best knowledge of the authors, no satisfactory solution to this problem has been published yet. On the other hand, as a result of the homogenization procedure, such difficulty is not met within the DCM approach. The only limitation is that the amplitude of the image force close to the surface may be smaller than the elastic prediction because of the smoothing of the shape functions.

Lastly, as emphasized by equation (14), the existence of elastic inclusions in the simulated body impose additional computations to the superposition approach and makes it less attractive by comparison to the DCM scheme, since the latter is transparent to this problem. As discussed in reference [1] and [12], in the case of the superposition approach, two-phase problems impose the calculation of the so-called polarization stresses in the inclusions,  $\hat{\rho} = (\underline{\underline{L}}^* - \underline{\underline{L}}) : \tilde{\underline{\underline{\epsilon}}} = (\underline{\underline{L}}^* : \underline{\underline{L}}^{-1} - \underline{\underline{I}}) : \tilde{\underline{\underline{\sigma}}}$ . Hence, the number of analytical calculations of the  $\tilde{\underline{\underline{\sigma}}}$  solutions at each step of the simulation is significantly increased (in addition to the boundary calculation, the stress field of each segments must be calculated at each Gauss points in  $V^*$ ).

## 5. Conclusion

In this paper, we provide a non-exhaustive list of advantages and disadvantages of the two numerical approaches used to solve boundary value problems in DD simulations, respectively the DCM and the superposition method. During these early stages of development of these simulation techniques, our aim was to draw the contour of their domains of excellence. Based on the comments made in §4, our recommendation to those starting in this field could be to try first the superposition method. This approach is easy to implement, delivers precise results and is efficient in terms of

CPU for simple problems. Then, for those interested in problems with a large density of dislocations and complex materials (e.g. multiphase materials, materials with strong elastic anisotropy materials, materials exhibiting plastic strain localization, ...) our preference would go to the second approach. Indeed, the DCM is numerically competitive (even faster) with large numbers of segments. Furthermore, with its concept of plastic strain homogenization, it provides an interesting self-consistent description of plasticity compatible with mesoscopic (discrete) and macroscopic (continuous) modeling of solid mechanics.

## 6. Acknowledgments

The authors wish to thank J-L. Chaboche, F. Feyel and L.P. Kubin for helpful discussions.

## References

1. E. Van der Giessen and A. Needleman, Model. Simul. Mater. Sci. Eng. **3**, 689 (1995).
2. D. Weygand, E. Van der Giessen and A. Needleman, Mat. Sci. Eng. **A309-310**, 420 (2001).
3. C.S. Shin, M.C. Fivel and K.H. Oh, J. Phys. IV France **11**, Pr5-27 (2001).
4. H. Yasin, H.M. Zbib and M.A. Khaleel, Mat. Sci. Eng. **A309-310**, 294 (2001).
5. C. Lemarchand, B. Devincre, L.P. Kubin and J.L. Chaboche, MRS Symposium Proceedings **538**, 63 (1999).
6. C. Lemarchand, Ph.D. Thesis, University of Paris VI (1999).
7. T. Mura, "Micromechanics of defects in solids", Second edition, Kluwer Academic Publishers (1993).
8. J.P. Hirth and J. Lothe, "Theory of dislocations", Second edition, John Wiley and Sons (1982).
9. C. Lemarchand, B. Devincre and L.P. Kubin, Journal of the Mechanics and Physics of Solids **49**, 1969 (2001).
10. D. Weygand, L.H. Friedman, E. Van der Giessen, A. Needleman, Model. and Simu. in Mat. Sci. and Eng. **10**, 437 (2002).
11. M.C. Fivel, T.J. Gosling and G.R. Canova Model. Simul. Mater. Sci. Eng. **4**, 581 (1996).
12. C.S. Shin, M.C. Fivel and K.H. Oh J. Phys. IV France **11**, 27 (2001).